Title	V2O3 polycrystalline nanorod cathode materials for Li-Ion batteries with long cycle life and high capacity retention
Authors	McNulty, David;Buckley, D. Noel;O'Dwyer, Colm
Publication date	2017-05-19
Original Citation	McNulty, D., Buckley, D. N. and O'Dwyer, C. (2017) 'V2O3 Polycrystalline Nanorod Cathode Materials for Li-Ion Batteries with Long Cycle Life and High Capacity Retention', ChemElectroChem, 4(8), pp. 2037-2044. doi: 10.1002/celc.201700202
Type of publication	Article (peer-reviewed)
Link to publisher's version	10.1002/celc.201700202
Rights	© 2017 Wiley-VCH Verlag GmbH & Co. KGaA, Weinheim. This is the peer reviewed version of the following article: D. McNulty, D. N. Buckley, C. O'Dwyer, 'V2O3 Polycrystalline Nanorod Cathode Materials for Li-Ion Batteries with Long Cycle Life and High Capacity Retention', ChemElectroChem 2017, 4, 2037, which has been published in final form at http://dx.doi.org/10.1002/celc.201700202. This article may be used for non-commercial purposes in accordance with Wiley Terms and Conditions for Self-Archiving.
Download date	2024-05-15 01:52:49
Item downloaded from	https://hdl.handle.net/10468/5480

V$_2$O$_3$ Polycrystalline Nanorod Cathode Materials for Li-ion Batteries with Long Cycle Life and High Capacity Retention

David McNulty[a], D. Noel Buckley[b],[c] and Colm O'Dwyer*[a],[d]

Abstract: We report on the electrochemical performance of V$_2$O$_3$ polycrystalline nanorods (poly-NRs) as a cathode material for Li-ion batteries. Poly-NRs are formed via thermal treatment of V$_2$O$_5$ nanotubes in a N$_2$ atmosphere. X-ray and electron diffraction are used to confirm the thermal reduction. Through galvanostatic cycling we demonstrate that poly-NRs offer excellent capacity retention over 750 cycles. The capacity retention from the 50th to the 750th cycle was an impressive ~ 94%, retaining a capacity of ~ 120 mAh g^{-1} after 750 cycles. The outstanding stability of the nanocrystal-containing V$_2$O$_3$ poly-NRs over many cycles demonstrates that vanadium(III) oxide (V$_2$O$_3$) performs very well as a cathode material. Full Li-ion cells with paired V$_2$O$_3$ poly-NR cathode and a pre-charged Co$_3$O$_4$ inverse opal conversion mode anode demonstrated high initial capacities and retained a capacity of 153 mAh g^{-1} after 50 cycles. The capacities achieved with our V$_2$O$_3$ poly-NRs/ Co$_3$O$_4$ IO full cells are comparable to the capacities obtained from the most commonly used cathode materials when cycled in a half cell arrangement versus pure Li metal.

Introduction

In recent years there has been an upsurge in the search for next generation Li-ion battery materials with higher capacities and increased energy densities. [1-5] Recently lithium-ion batteries have penetrated the market of hybrid and electrical vehicles [6, 7] and continue to dominate the market for handheld electronic devices. Over the last decade the technological advancements which have led to these products have been outstanding and currently battery technology is just about keeping up. With the power and energy demands of future technological advancements, every aspect of Li-ion batteries must be developed and enhanced. There is a tremendous amount of research being made into possible cathode materials to replace the most commonly currently used cobalt oxides. [8-10]

[a]   Dr D. McNulty, Dr C. O'Dwyer
        Department of Chemistry, University College Cork, Cork,
        T12 YN60, Ireland
        *E-mail: c.odwyer@ucc.ie
[b]   Prof. D. N. Buckley
        Department of Physics and Energy, University of Limerick, Limerick,
        V94 T9PX, Ireland
[c]   Prof. D. N. Buckley
        Bernal Institute, University of Limerick, Limerick, V94 T9PX, Ireland
[d]   Dr C. O'Dwyer
        Micro-Nano Systems Centre, Tyndall National Institute, Lee
        Maltings, Cork, T12 R5CP, Ireland

        Supporting information for this article is given via a link at the end of the document.

Vanadium oxide nanotubes (VONTs) were first reported in 1998 by Spahr et al. [11] based on related soft chemistry approaches pioneered by Livage and colleagues [12, 13], and since then has been a great deal of research into how to fully optimise them as a cathode material for Li-ion batteries. [14-20] Typically VONTs are prepared by hydrothermal treatment of a vanadium oxide precursor mixed with a primary amine. [21-23] The amine molecules are a crucial component of the VONT synthesis as they maintain the vanadium oxide layers which scroll to form the nanotube structure. [24, 25] Despite the structure defining role of the amines in the synthesis of the VONTs, they are detrimental to their electrochemical performance.[26] We have previously reported on the poor electrochemical performance of as prepared VONTs, which achieved capacities < 10 mAh g^{-1}.[27] We demonstrated that the amine molecules which occupy the majority of the possible lithium intercalation sites within the VONTs are responsible for the poor cycling performance and that removing the amines via thermal treatment can significantly improve electrochemical performance. While as-synthesised VONTs exhibit poor electrochemical performance, they are quite useful in providing nanorod or nanowire-type structures with nanoscale features after various post-treatments. Thermal treatment of VONTs in a N$_2$ atmosphere results in a specific structural conversion V$_2$O$_5$ to V$_2$O$_3$ polycrystalline nanorods (poly-NRs) during annealing.[27] Previous studies have detailed the reduction of various V$_2$O$_5$ samples to V$_2$O$_3$ via annealing in inert atmospheres, such as the reduction of a V$_2$O$_5$ gel via annealing in H$_2$ and the formation of V$_2$O$_3$ nanocrystals by thermal reduction of V$_2$O$_5$ thin films. [28, 29]

Interestingly, V$_2$O$_3$ has previously been reported as both a cathode and an anode material, depending upon the potential windows investigated. [30-33] One of the earliest papers on the electrochemical performance of V$_2$O$_3$ reported promising capacities for a V$_2$O$_3$@C composite cycles as a cathode material [30] however since this report there have been a number of studies on the application of V$_2$O$_3$ nanostructures as an anode material with varying levels of success. Reported capacity values for V$_2$O$_3$ nanostructures cycled as an anode material can vary wildly. V$_2$O$_3$ nanorods delivered a capacity of ~50 mAh g^{-1} after 100 cycles at 0.1 C [34], whereas composites of V$_2$O$_3$ nanoparticles with carbon have been reported to deliver a capacity of ~780 mAh g^{-1} after 100 cycles at 0.2 C.[35] It is worth noting that the V$_2$O$_3$/C composite was cycled in a potential window of 3.0 – 0.01 V, and carbon is electrochemically active toward intercalation in this potential window, and so may also be contributing to the increased capacity. The significant variation in reported capacity values may indicate the instability of V$_2$O$_3$ as an anode material. Vanadium oxides have been the subject of much research as Li-ion battery materials due to the multiple oxidation states of vanadium. Previous reports investigating the electrochemical performance of V$_2$O$_5$ as a cathode material

have used a potential window of 4.0 – 1.2 V [21, 36], which is quite a low potential window considering that TiO_2 anode materials are typically cycled from 3.0 – 1.0 V [37, 38], demonstrating that there can be crossover in the potential windows used for cathode and anode materials.

In this report we detail the ability to prepare V_2O_3 in nanorod form with high grain boundary content, directly from highly ordered scrolled V_2O_5 nanotubes, for Li-ion cathode applications. Analysis of X-ray and electron diffraction patterns confirms that the nanorods are phase pure rhombohedral V_2O_3. The electrochemical performance of the V_2O_3 poly-NRs is evaluated via cyclic voltammetry, rate capability testing and long cycle life galvanostatic tests. To our knowledge the specific capacity results presented in this report, represent one of the best electrochemical performances ever reported for V_2O_3 as a cathode material. We demonstrate stable cycling of the poly-NRs over 750 cycles at 0.4 C. The electrochemical performance of the V_2O_3 poly-NRs as a cathode material was further evaluated by galvanostatic cycling in a full cell configuration against a pre-charged Co_3O_4 inverse opal (IO) anode. Three-dimensional ordered macroporous (3DOM) electrode materials such as IOs have previously been reported to increase cycling stability and capacity retention for various transition metal oxides. [39-41] To our knowledge this report represents the first time a V_2O_3 nanostructure has been paired with a conversion mode anode material to prepare a full Li-ion cell. The V_2O_3 poly-NRs/ Co_3O_4 IO full cell demonstrated promising Li$^+$ insertion activity, accommodating up to $Li_{0.85}V_2O_3$ and $Li_{0.66}V_2O_3$ after 50 and 100 cycles, respectively, when cycled at 1 C. We demonstrate that the specific capacity values achieved from the V_2O_3 poly-NRs cycled in a full cell are higher than previously reported values for V_2O_3 nanostructures cycled against pure Li metal in a half cell arrangement. The discharge capacity obtained for our full cells after 50 cycles (153 mAh g^{-1}) is comparable to the initial capacities obtained for the most commonly used cathode materials ($LiCoO_2$, $LiMn_2O_4$) when cycled in half cell against pure Li metal.

Results and Discussion

V_2O_3 polycrystalline nanorods (poly-NRs) were prepared via thermal treatment of nonylamine containing vanadium oxide nanotubes (VONTs) in a nitrogen atmosphere to ensure a high nanocrystalline and grain boundary content in the reconstructed morphology; the tube aspect ratio is maintained, but internal layered structure is modified to monocrystalline grains. A schematic representation of the conversion from a highly ordered VONT to a poly-NR is shown in Figure 1a. Initially as prepared VONTs are scrolled nanotubes with a hollow core, layered walls and well-defined tube openings, as shown in Figure 1b. Nonylamine molecules intercalated between layers of vanadium oxide facilitate scrolling during hydrothermal treatment to form the scrolled VONTs. Heating the VONTs to 600 °C, removes the structure-maintaining amine template, and results in the structural conversion to poly-NRs. Figure 1c demonstrates

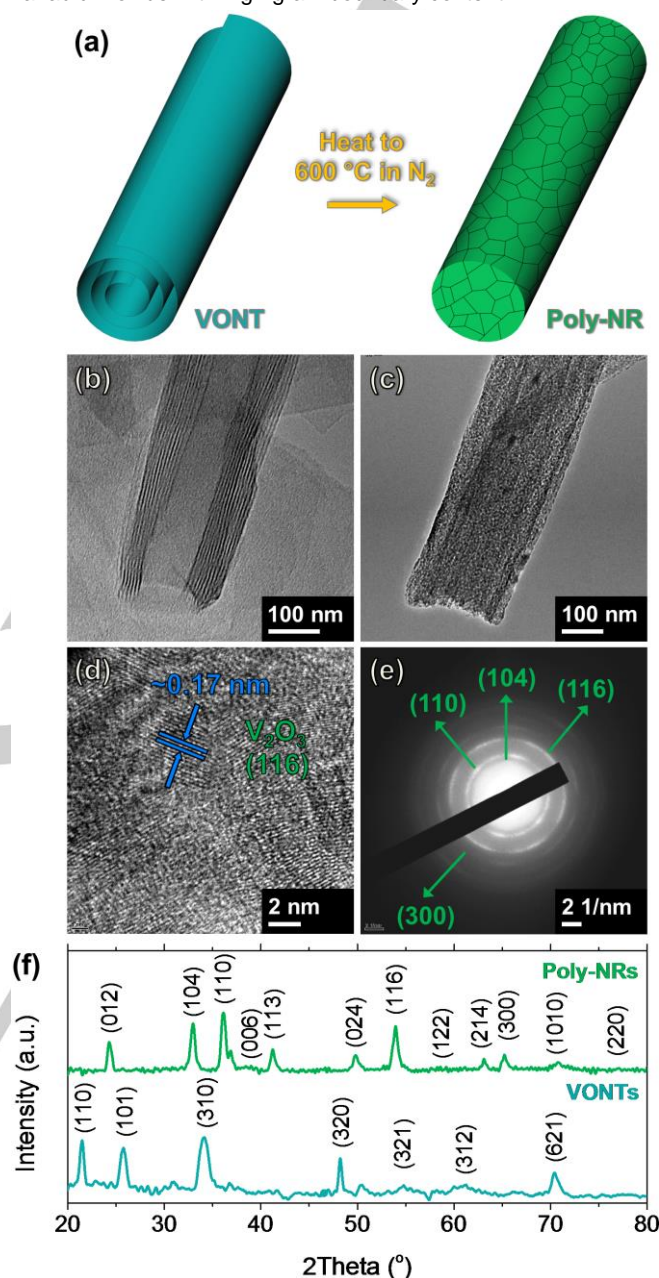that poly-NRs are an agglomeration of nanocrystallites of vanadium oxide with high grain boundary content.

Figure 1. (a) Schematic representation of the structural conversion from a highly ordered vanadium oxide nanotube to a polycrystalline nanorod via annealing to 600 °C in N_2. TEM images of (b) an individual VONT and (c) V_2O_3 poly-NR. (d) High magnification TEM image showing the lattice fringes of a typical poly-NR. (e) Electron diffraction pattern of a typical V_2O_3 poly-NR. (f) XRDs pattern for VONTs and poly-NRS.

The lattice fringes of the poly-NRs, shown in Figure 1d, have a spacing of ~0.17 nm, corresponding to the (116) plane for rhombohedral V_2O_3. The electron diffraction (ED) pattern for a typical poly-NR consists of a series of diffraction rings

indicating its polycrystalline structure, as shown in Figure 1e. The ED pattern was successfully indexed to pure rhombohedral V_2O_3. XRD analysis was used in order to confirm the phase of the poly-NRs, the XRD patterns for VONTs and poly-NRs are shown in Figure 1f. The reflections observed can be indexed to pure orthorhombic V_2O_5 (JCPDS No. 98-000-6042) with a Pmnn space group and pure rhombohedral V_2O_3 (JCPDS No. 01-1293) with an R-3c space group, respectively.

To evaluate the electrochemical performance of the poly-NRs as a cathode material, a sample was charged and discharged galvanostatically for 750 cycles, in a potential window from 4.0 – 1.2 V, using a C-rate of 0.4 C. A selection of the resulting charge and discharge curves ranging from the 1st to the 750th cycle is shown in Figure 2a-c. The initial discharge curve consisted of two sloping regions centred at ~ 1.9 and 1.3 V as shown in Figure 2a. To further investigate the origin of these sloping regions, a differential charge plot was calculated for the first galvanostatic charge curve. Two peaks can be seen in the differential capacity curve, as shown in the inset in Figure 2a. The broad peak centred at 2.00 V and the strong peak at 1.35 V have previously been observed for other V_2O_3 nanostructures and are associated with the reduction of V^{3+}.[31, 42] XPS analysis of a poly-NR sample before and after the first discharge is presented in the supporting information. It has been reported in cases where V_2O_3 was treated as an anode material, that a full charge to a lower voltage limit of 0.01 V resulted in the reduction of V^{3+} to metallic vanadium, [35, 43] however in this study

poly-NR V_2O_3 material forms a lithiated vanadate in which the vanadium is in higher oxidation states (V^4 and V^{5+}). The specific capacity after the first discharge was ~ 560 mAh g^{-1}, which is significantly higher than the theoretical capacity for V_2O_3 (179 mAh g^{-1} for $Li_1V_2O_3$); XPS detected composition consistent with Li_3VO_4. The large initial discharge capacity may also comprise contributions from defects such as cation vacancies associated with lithiated oxygen sites, which may form during the preparation of the poly-NRs. It has previously been reported that point defects may be introduced into V_2O_5 via heat treatment and these defects can serve as additional charge-storage sites, resulting in large initial capacities.[44] Consequently, the presence of any such defects may also partially contribute to the irreversible capacity loss after the first charge. V_2O_3 poly-NRs are prepared via a reduction of V_2O_5 VONTs via thermal treatment in N_2, which may lead to the formation of similar defect sites.

After the 2nd discharge ~1.09 mol of Li per V_2O_3 unit was inserted into the poly-NR cathode and ~0.93 mol of Li was removed upon the second charge, indicating that the insertion and removal of Li$^+$ was much more reversible after the 1st cycle. We observed little variation in the number of moles of lithium inserted from the 50th to the 750th charges, decreasing slightly from ~0.70 to 0.66 mol. This indicates that the insertion and removal of Li$^+$ is highly reversible for the V_2O_3 poly-NRs. The sloping regions observed in the first discharge curve can be seen in the various discharge curves shown in Figure 2a-c.
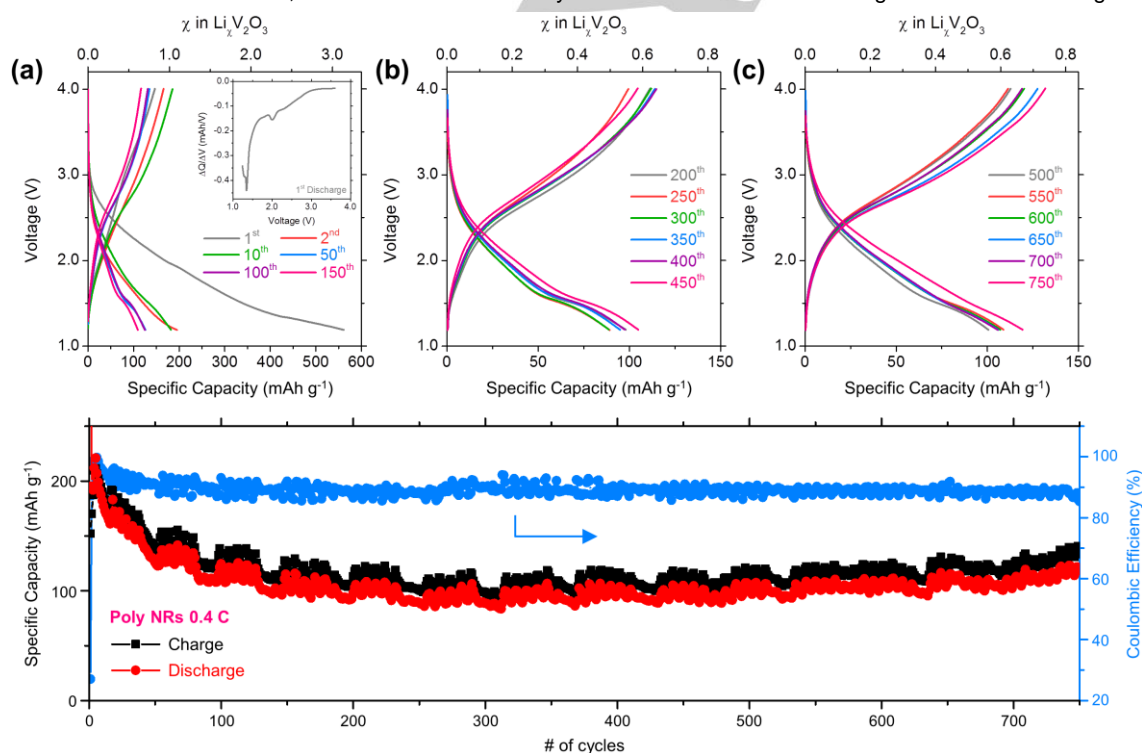
the V_2O_3 poly-NR samples are discharged to 1.20 V and the

Figure 2. Charge and discharge voltage profiles for (a) the 1st, 2nd, 10th, 50th, 100th and 150th cycles, (b) the 200th, 250th, 300th, 350th, 400th, and 450th cycles and (c) the 500th, 550th, 600th, 650th, 700th and 750th cycles for V_2O_3 poly-NRs at a C-rate of 0.4 C in a potential window of 4.0 – 1.2 V (vs Li/Li$^+$). (d) Comparison of the specific capacity values and coulombic efficiency obtained for V_2O_3 poly-NRs over 750 cycles.

To further investigate the reversibility of the insertion and removal of Li+ differential charge curves for a series of discharge curves ranging from the 100th to the 750th discharge were calculated, as shown in Figure S2 (Supporting Information). The strong reduction peak at 1.35 V in the differential charge curve for the 1st discharge was shifted to a higher potential (1.55 V) and the broad peak centred at 2.00 V became much broader after the 100th discharge. This shift to higher potentials for the strong reduction peak after the first cycle is likely due to a decrease in particle size. The poly-NRs are comprised of an agglomeration of nanoparticles. The decrease in particle size may be due to the insertion and removal of Li+ during the first cycle and is commonly referred to as "electrochemical grinding" of the initial material. [45] There was slight variation in the potential of the strong reduction peak from the 100th to the 400th discharge however after the 400th discharge the centre of the reduction peak remained at 1.55 V. After the 500th discharge the reduction peak shifted slightly to 1.51 V and decreased in potential further to 1.43 V after the 750th discharge. The presence of the strong reduction peak in the differential charge curves even after 750 cycles and the slight variation in the potential of the reduction peak from the 100th to the 750th discharge suggests that the insertion and removal of Li+ is a highly reversible process for our V_2O_3 poly-NRs. While V_2O_5 is well known to have a van der Waals layered structure to accommodate cation insertion, the high grain boundary content in V_2O_3 likely facilitates the stable reversible lithiation with extended cycling.
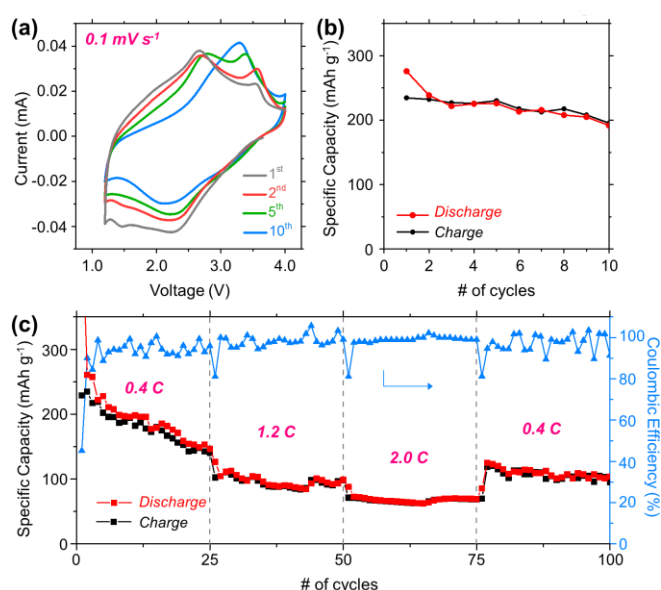

Figure 3. (a) Cyclic voltammograms for V_2O_3 poly-NRs, acquired at a scan rate of 0.1 mV s^{-1}. (b) Discharge and charge capacities calculated from cyclic voltammograms. (c) Rate capability test for V_2O_3 poly-NRs over 100 cycles, using C-rates ranging from 0.4 C to 2.0 C.

The specific capacity values obtained for the poly-NRs at 0.4 C and their related coulombic efficiency values are shown in

Figure 2d. It can be clearly seen that the V_2O_3 poly-NRs offer excellent capacity retention as a cathode material over 750 cycles. After ~50 cycles the high initial capacities begin to level off after that the capacity retention was exceptionally high for the remainder of the 750 cycles. The discharge capacity after the 2nd cycle was 195 mAh g^{-1}, this decreased to 182 mAh g^{-1} after the 10th cycle and to 156 mAh g^{-1} after the 25th cycle. There was little diminution in the discharge capacities from the 50th to the 750th cycles having capacities of 126 and 119 mAh g^{-1}, respectively. This corresponds to a capacity retention of ~ 94% from the 50th to the 750th cycle. This level of capacity retention demonstrates the stability of the V_2O_3 poly-NRs when cycled as a cathode material. The specific capacity values obtained for V_2O_3 poly-NRs are comparable to previously reported values for other vanadium oxide nanostructured cathode materials including V_2O_5 nanosheets [46], V_2O_5/PEDOT/MnO_2 nanowires [47] and $VO_{2.07}$/RGO composite films. [48]

To our knowledge our results represent one of the best electrochemical performances ever reported for V_2O_3 as a cathode material. While the coulombic efficiency is quite low, it maintains a consistent level over 750 cycles and the cause is the high upper limit of the discharge curve. Otherwise, the material is very efficient in each cycle. There are a small number of reports detailing the electrochemical performance of V_2O_3 as an anode material however the results presented in Figure 2 demonstrate the viability of V_2O_3 as a cathode material for Li and Li-ion batteries. The periodic undulation observed in the specific capacity in Fig. 2d can be attributed to temperature differences during long term cycling. Figure S3 (Supporting Information) demonstrates the influence of temperature on the specific capacity values obtained over a 24 h period from the 700th to 707th cycles. The highest discharge capacities were obtained when the temperature was at its highest, but the intermittent variation did not affect the stable capacity and retention over the full cycle life test - the material without binder or conductive additive is very stable. An increase in specific capacity values from the 400th cycle onwards was observed in Figure 2d. The capacity rise after prolonged cycling has been observed for other V_2O_3 samples and has been attributed to a possible activation process, in which previously electrochemically inactive regions become exposed due to progressive pulverization resulting from electrochemical grinding effects. [35, 43, 49, 50] Consequently the intercalation of Li+ into these newly exposed regions result in higher specific capacities.

The electrochemical performance of the poly-NRs was further investigated via cyclic voltammetry as shown in Figure 3a. We have previously reported on the use of cyclic voltammetry to distinguish the charge stored due to lithium intercalation processes from extrinsic capacitive effects for V_2O_3 poly-NRs and determined that ~83% of the charge stored can be attributed to the contribution due to intercalation processes. [51] A broad peak and a more discrete weak peak were observed in the first cathodic sweep centred at ~2.28 and 1.44 V, respectively, which are in close agreement with the two peaks observed in the differential charge curve for the first discharge. In subsequent cycles the broad peak shifted to ~ 2.16 V and the discrete peak was no longer observed. The first anodic sweep consisted of a

strong peak at 2.67 V and a weaker peak at 3.55 V, corresponding to the reoxidation of vanadium due to change in phase from the lithiated vanadate to an oxide. [43] We have previously reported on the pseudocapacitive charge storage of poly-NRs and found that up to ~17% of the charge stored at a scan rate of 0.1 mV/s can be attributed to capacitive surface charge storage but under potentiodynamic conditions. [51] The specific capacities determined from the CV curves for 10 cycles at a scan rate of 0.1 mV s^{-1} are shown in Figure 3b. The initial discharge capacity was 276 mAh g^{-1}, this decreased slightly to 226 mAh g^{-1} after the 5th cycle and decreased further to 192 mAh g^{-1} after the 10th cycle. These capacity values are in close agreement with the values from galvanostatic testing, presented in Figure 2d.

The capacity retention of V$_2$O$_3$ poly-NRs samples was further investigated by rate capability testing using series of different charge rates ranging from 0.4 – 2.0 C. The specific capacity obtained after 25 cycles at 0.4 C was ~146 mAh g^{-1}. The average discharge capacity over 25 cycles obtained at 1.2 C was ~98 mAh g^{-1} and this value decreased to 68 mAh g^{-1} at highest C-rate used (2.0 C). However, when the charge rate was returned to the initial value of 0.4 C the specific capacity recovered to 125 mAh g^{-1}. This corresponds to a recovery of ~86% of the capacity after the 25th cycle at 0.4 C. From the capacity values achieved during the galvanostatic test present in Figure 2d and the rate capability test in Figure 3c, the V$_2$O$_3$ poly-NRs as cathode materials demonstrate significant reversible capacity, stable capacity retention and rate performance.

To further evaluate the performance of the V$_2$O$_3$ poly-NRs as a cathode material, full Li-ion cells were prepared consisting of a poly-NR cathode and an electrochemically pre-lithiated Co$_3$O$_4$ inverse opal (IO) anode. The theoretical capacity of Co$_3$O$_4$ (890 mAh g^{-1}) is higher than that of V$_2$O$_3$ (179 mAh g^{-1}), as a proof of concept, the Co$_3$O$_4$ IO anode was prelithiated so as to have an excess of Li in our full cell system. A schematic representation of these full cells is illustrated in Figure 4a. We have previously reported on the impressive performance of Co$_3$O$_4$ IO anodes in half cells cycled against Li metal [52] and in a full cell arrangement when paired with V$_2$O$_5$ IO cathodes. [53] To our knowledge this study represents the first report on a full Li-ion cell consisting of a V$_2$O$_3$ cathode paired with a conversion mode anode material. SEM images of the poly-NRs and a Co$_3$O$_4$ IO sample are shown in Figure 4b and c, respectively. The diameter of the V$_2$O$_3$ poly-NRs is ~150 nm with lengths up to ~1 µm as shown in Figure 4b. Co$_3$O$_4$ IOs were prepared via infilling of a sacrificial polystyrene sphere (PS) template with a 0.1 M CoCl$_2$ solution on a stainless steel substrate. The samples were then annealed at 450 °C for 12 h to remove the PS sphere template and to crystallize the cobalt oxide samples. The walls of the IO structure are comprised of an agglomeration of nanoscale crystallites of Co$_3$O$_4$ and the pores of the IO are < 500 nm as shown in Figure 4c, and the material is electrically interconnected throughout the coating.

Co$_3$O$_4$ IOs were pre-lithiated via charging in a half cell configuration against a Li metal counter electrode, prior to being paired with V$_2$O$_3$ poly-NRs cathodes. A full Li ion cell consisting of a V$_2$O$_3$ poly-NRs cathode and a pre-charged Co$_3$O$_4$ IO anode

was cycled for 100 cycles at a 1 C and a selection of the resulting charge and discharge profiles are shown in Figure 5a and b. The specific capacity values and the C-rate values presented were calculated in terms of the mass of the cathode. The OCV for the V$_2$O$_3$ poly-NRs half cells was ~ 3.6 V (vs Li/Li$^+$), however the OCV for the V$_2$O$_3$ poly-NRs/ Co$_3$O$_4$ IO cell the OCV was ~ 2.6 V. Due to this decrease in the OCV, the potential window used for the full cell was 3.0 – 0.2 V. We have previously reported a similar shift in potential window for V$_2$O$_5$ IO/Co$_3$O$_4$ IO full cells and V$_2$O$_5$ IO/Ni-Mn-Co-O IO full cells. [53, 54]
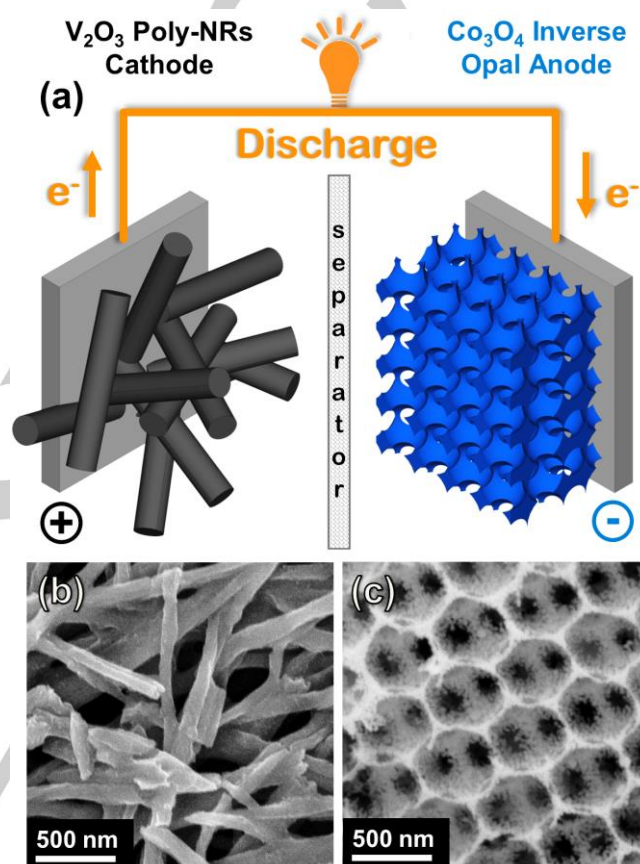

Figure 4. (a) Schematic representation of a two electrode Li-ion cell consisting of a V$_2$O$_3$ poly-NRs cathode and a prelithiated Co$_3$O$_4$ IO anode. SEM images of (b) V$_2$O$_3$ poly-NRs and (c) a Co$_3$O$_4$ IO.

The voltage profiles for the V$_2$O$_3$ poly-NRs/ Co$_3$O$_4$ IO full cell are smooth curves without any discrete voltage steps as shown in Figure 5a and b. This may be due to the full cells being cycled in a 2 electrode configuration. Without a dedicated reference electrode the first discharge curve for the full cell is a convolution of the first discharge for the V$_2$O$_3$ poly-NRs cathode and the first discharge of the Co$_3$O$_4$ IO anode. To further investigate the electrochemical processes occurring during charging and discharging, differential capacity curves for a range of cycles from the 1st to the 100th were determined from the voltage profiles shown in Figure 5a and b, as shown in Figure S4. The differential charge curve from the 1st discharge shown in Figure S4a consisted of a sharp peak at ~1.68 V and a wide

peak centred at ~1.08 V. The wide peak was shifted to a higher potential of ~1.40 V for the 2nd discharge and the intensity of this peak gradually faded over the remainder of the 100 cycles, corresponding to the capacity fade observed in Figure 5c. The differential charge curve for the 1st discharge consisted of a wide peak at ~1.73 V and again the intensity of this peak faded with increased cycling. As discussed the voltage profiles for the V_2O_3 poly-NRs/ Co_3O_4 IO cells are a convolution of the electrochemical responses of the poly-NR cathode and the Co_3O_4 IO anode due to cycling in a 2-electrode configuration. Therefore, it is difficult to assign the resulting peaks observed in the differential charge curves to a specific process involving the insertion/removal of Li^+ for either one of the electrode materials.
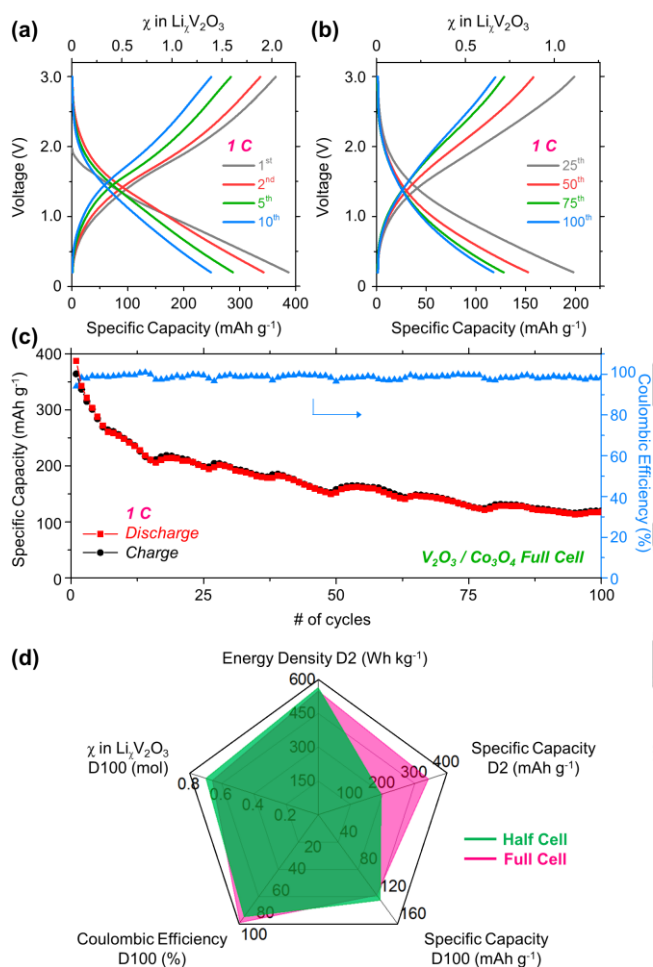
After the first discharge 2.16 mol of Li was intercalated into the V_2O_3 cathode from the Co_3O_4 IO anode. This value decreased slightly to 1.92 mol after the 2nd discharge and decreased further to 1.39 mol after the 10th discharge. After the 50th discharge this value decreased to 0.85 mol and after the 100th discharge 0.66 mol of Li was intercalated. The gradual decrease in the amount of Li per V_2O_3 unit with increased cycling is comparable to the performance of the V_2O_3 poly-NRs presented in Figure 2. During cycling, Li ions may become trapped between layers of vanadium oxide within regions of the poly-NRs due to a local collapsing of the layers. This reduces the maximum amount of lithium which may be reversibly intercalated and consequently results in capacity fading. [19] However, in a full cell configuration the nature of the conversion mode reaction which the Co_3O_4 IO anode undergoes may also be contributing to the gradual decrease in intercalated Li^+. After the initial charging of the Co_3O_4 anode in a half cell configuration, Co and Li_2O are formed.[55, 56] During the first discharge in our V_2O_3 poly-NRs/ Co_3O_4 IO full cells, these products are oxidized to form CoO and Li^+. The efficiency of this conversion mode reaction likely dictates the efficiency of the overall full cell.

The specific capacity values obtained for the V_2O_3 poly-NRs/ Co_3O_4 IO full cell over 100 cycles and the corresponding coulombic efficiencies are shown in Figure 5c. The initial high discharge capacity of 387 mAh g^{-1} decreased to 221 mAh g^{-1} after the 15th discharge and from that cycle onwards there was a far more gradual decrease in the capacity values. After the 50th discharge the capacity was 153 mAh g^{-1} and this decreased to 118 mAh g^{-1} after the 100th cycle. The capacity values obtained are significantly higher that previously reported values for V_2O_3 nanostructures tested as a cathode material, including V_2O_3 spheres, nanobelts and V_2O_3@C composites.[30] The capacity values obtained for the V_2O_3 poly-NRs/ Co_3O_4 IO full cell after 50 cycles (~153 mAh g^{-1}) are comparable to the initial capacities for the most commonly used cathode materials cycled in a half cell configuration, such as $LiCoO_2$, $LiMn_2O_4$, $LiFePO_4$ and $LiNi_{1/3}Co_{1/3}Mn_{1/3}O_2$. [57-60]

Reports on the performance of full Li ion cells remain uncommon in the literature with most reports focused on half-cell performance. Here we report on a functioning full Li ion cell with capacities comparable to the most commonly investigated cathode materials cycled against Li metal. The V_2O_3 poly-NRs/ Co_3O_4 IO full cell also offered good coulombic efficiencies having a value of > 95% from the second cycle onwards. The promising capacities achieved from the V_2O_3 poly-NRs/ Co_3O_4 IO full cell demonstrate the importance of investigating non-traditional pairings of high performance battery electrode materials for full Li-ion cells. Identifying suitable electrode pairings and cycling in a full cell arrangement is important for advancing Li-ion battery technology. A comparison of the electrochemical performance for poly-NR samples cycled in a half cell configuration against Li metal and cycled in a full cell against a pre-charged Co_3O_4 IO anode is shown in Figure 5d. The calculated energy density for the poly-NRs cycled in a full Li-ion cell (549 Wh kg^{-1}) is comparable to the energy density for poly-NRs cycled against Li metal (563 Wh kg^{-1}). Except for the specific capacity after the second discharge, the overall

Figure 5. Charge and discharge voltage profiles for (a) the 1st, 2nd, 5th and 10th cycles and (b) the 25th, 50th, 75th and 100th cycles for a V_2O_3 poly-NRs/ Co_3O_4 IO full cell at a C-rate of 1 C in a potential window of 3.0 – 0.2 V. (c) Comparison of the specific capacity values and coulombic efficiency obtained for a V_2O_3 poly-NRs/ Co_3O_4 IO full cell over 100 cycles. (d) Radar plots comparing the energy density, specific capacity, coulombic efficiency and number of moles of Li intercalated for V_2O_3 poly-NRs cycled in a half cell configuration against Li metal and cycled in a full cell against a pre-charged Co_3O_4 IO anode. D2 and D100 refer to the 2nd and 100th discharge.

performance of poly NRs in a full Li-ion cell paired with a pre-charged Co_3O_4 IO anode is in close agreement with the values obtained in a half cell cycled against Li metal. Achieving values when cycled in a full cell which are comparable to values obtained in a half cell, demonstrates the stability of the poly-NR anode material.

Conclusions

V_2O_3 poly-NRs with high grain boundary content were prepared via thermal treatment of highly ordered scrolled VONTs in a N_2 atmosphere. Electron diffraction and X-ray diffraction confirm the thermal reduction from V_2O_5 to V_2O_3. Nanostructures of V_2O_3 have previously been reported as both a cathode and an anode material. Through galvanostatic cycling we demonstrate that V_2O_3 poly-NRs offer excellent capacity retention as a cathode material over 750 cycles. Little variation was observed in the discharge capacities from the 50th to the 750th cycles, having values of 126 and 119 mAh g^{-1}, respectively, corresponding to a capacity retention of ~ 94%. The capacity values obtained when cycled 750 times at a 0.4 C are greater than previously reported values for other vanadium oxide nanostructures. The impressive stability of the V_2O_3 poly-NRs over a large number of cycles confirm the sesquioxide phase of V_2O_3 is a useful cathode material. Rate capability tests of the poly-NRs demonstrated significant reversible capacity of ~ 125 mAh g^{-1}, considerable capacity retention after 100 cycles and outstanding rate performance.

To further emphasise the functionality of the V_2O_3 poly-NRs as a cathode, full cells comprised of a poly-NR cathode and a pre-charged Co_3O_4 IO anode were prepared. To our knowledge this report represents the first time a V_2O_3 nanostructure has been paired with a conversion mode anode material. The V_2O_3 poly-NRs/ Co_3O_4 IO full cell demonstrated high initial capacities and retained a capacity of 153 mAh g^{-1} after 50 cycles. The capacities obtained from the V_2O_3 poly-NRs/ Co_3O_4 IO full cell are comparable to the capacities obtained when the poly-NRs were cycled against Li metal and for the most commonly used cathode materials when cycled in a half cell configuration. The impressive electrochemical performance of the V_2O_3 poly-NRs demonstrates that they are a very promising cathode material for further development and application in long cycle life Li-ion batteries.

Experimental Section

Preparation of V_2O_3 poly-NRs

V_2O_3 poly-NRs were prepared by annealing vanadium oxide (V_2O_3 nanotubes (VONTs) as previously reported.[27] Briefly, VONTs were synthesised via hydrothermal treatment of a vanadium oxide xerogel mixed with nonylamine. The as-prepared VONTs were then annealed to 600 °C in a nitrogen atmosphere, resulting in a structural conversion from V_2O_5 VONTs to V_2O_3 poly-NRs.

Preparation of Co_3O_4 inverse opals

Co_3O_4 IO samples were prepared *via* infilling of a polystyrene (PS) sphere template. Initially a solution of PS spheres (Polysciences Inc., diameter = 500 nm) in isopropanol (IPA) was drop cast on to 1 cm^2 pieces of stainless steel; the sphere templates were then infilled with a 0.1 M solution of $CoCl_2$ in IPA. The infilled sphere templates where heated at 450 °C in air for 12 h, to remove the templates and to crystallize the samples.

Material Characterization

TEM analysis was conducted using a JEOL JEM-2100 TEM operating at 200 kV. SEM analysis was performed using an FEI Quanta 650 FEG high resolution SEM at an accelerating voltage of 10 kV. XRD analysis was performed using a Phillips Xpert PW3719 diffractometer using Cu Kα radiation. (Cu Kα, λ = 0.15418 nm, operation voltage 40 kV, current 40 mA).

Electrochemical Characterization

All electrochemical results presented in this report were performed using a BioLogic VSP Potentiostat/Galvanostat. The electrochemical properties of V_2O_3 poly-NR samples were investigated in a half cell configuration against a pure Li counter electrode in a two electrode, stainless steel split cell (a coin cell assembly that can be disassembled for post-mortem analysis). The electrolyte used consisted of a 1 mol dm^{-3} solution of lithium hexafluorophosphate salt in a 1:1 (v/v) mixture of ethylene carbonate in dimethyl carbonate with 3 wt% vinylene carbonate. The separator used in all split cell tests was a glass fiber separator (El-Cell ECC1-01-0012-A/L, 18 mm diameter, 0.65 mm thickness). The mass loading for all V_2O_3 poly-NR samples was ~ 0.5 – 1.0 mg, no additional conductive additives or binders were added. Cyclic voltammetry was performed using a scan rate of 0.1 mV s^{-1} in a potential window of 4.0 – 1.2 V (vs Li/Li+). Galvanostatic cycling of the V_2O_3 poly-NR half cells was performed using a range of C rates in a potential window of 4.0 – 1.2 V (vs Li/Li+). For testing in a full cell arrangement against a V_2O_3 poly-NR cathode, the Co_3O_4 IO anode was electrochemically pre-charged by a single charge against a Li metal counter electrode. The mass loading for typical Co_3O_4 samples was ~ 0.75 mg. The V_2O_3 poly-NRs/ Co_3O_4 IO full cells were galvanostatically cycled in a 2 electrode configuration with the pre-charged Co_3O_4 IO anodes serving as both the anode and reference electrode in potential window of 3.0 – 0.2 V.

Acknowledgements

[1] P. G. Bruce, B. Scrosati, J.-M. Tarascon, Angew. Chem. Int. Ed. 2008, 47, 2930.

[2] M. Hu, X. Pang, Z. Zhou, J. Power Sources 2013, 237, 229.

[3] N. Nitta, F. Wu, J. T. Lee, G. Yushin, Mater. Today 2015, 18, 252.

[4] P. Rozier, J. M. Tarascon, J. Electrochem. Soc 2015, 162, A2490.

[5] P. Roy, S. K. Srivastava, J. Mater. Chem. A 2015, 3, 2454.

[6] L. Lu, X. Han, J. Li, J. Hua, M. Ouyang, J. Power Sources 2013, 226, 272.

[7] E. Karden, S. Ploumen, B. Fricke, T. Miller, K. Snyder, J. Power Sources 2007, 168, 2.

[8] D. Liu, W. Zhu, J. Trottier, C. Gagnon, F. Barray, A. Guerfi, A. Mauger, H. Groult, C. Julien, J. Goodenough, RSC Adv. 2014, 4, 154.

[9] B. Xu, D. Qian, Z. Wang, Y. S. Meng, Mater. Sci. Eng. R-Rep. 2012, 73, 51.

[10] B. Wang, B. Xu, T. Liu, P. Liu, C. Guo, S. Wang, Q. Wang, Z. Xiong, D. Wang, X. S. Zhao, Nanoscale 2014, 6, 986.

[11] M. E. Spahr, P. Bitterli, R. Nesper, M. Müller, F. Krumeich, H. U. Nissen, Angew. Chem. Int. Ed. 1998, 37, 1263.

[12] J. Livage, Chem. Mater. 1991, 3, 578.

[13] J. Livage, Materials 2010, 3, 4175.

[14] S. Nordlinder, K. Edström, T. Gustafsson, Electrochem. Solid State Lett. 2001, 4, A129.

[15] S. Nordlinder, L. Nyholm, T. Gustafsson, K. Edström, Chem. Mater. 2005, 18, 495.

[16] C.-j. Cui, G.-m. Wu, J. Shen, B. Zhou, Z.-h. Zhang, H.-y. Yang, S.-f. She, Electrochim. Acta 2010, 55, 2536.

[17] H. X. Li, L. F. Jiao, H. T. Yuan, M. Zhang, J. Guo, L. Q. Wang, M. Zhao, Y. M. Wang, Electrochem. Commun. 2006, 8, 1693.

[18] Z. Li, G. Liu, M. Guo, L.-X. Ding, S. Wang, H. Wang, Electrochim. Acta 2015, 173, 131.

[19] D. McNulty, D. N. Buckley, C. O'Dwyer, J. Power Sources 2014, 267, 831.

[20] C. O'Dwyer, V. Lavayen, D. A. Tanner, S. B. Newcomb, E. Benavente, G. Gonzalez, E. Benavente, C. M. S. Torres, Adv. Funct. Mater. 2009, 19, 1736.

[21] M. E. Spahr, P. Stoschitzki Bitterli, R. Nesper, O. Haas, P. Novák, J. Electrochem. Soc 1999, 146, 2780.

[22] H. J. Muhr, F. Krumeich, U. P. Schönholzer, F. Bieri, M. Niederberger, L. J. Gauckler, R. Nesper, Adv. Mater. 2000, 12, 231.

[23] D. McNulty, D. N. Buckley, C. O'Dwyer, ECS Trans. 2011, 35, 237.

[24] F. Krumeich, H. J. Muhr, M. Niederberger, F. Bieri, B. Schnyder, R. Nesper, J. Am. Chem. Soc 1999, 121, 8324.

[25] M. Niederberger, H.-J. Muhr, F. Krumeich, F. Bieri, D. Günther, R. Nesper, Chem. Mater. 2000, 12, 1995.

[26] D. McNulty, D. N. Buckley, C. O'Dwyer, ECS Trans. 2013, 50, 165.

[27] D. McNulty, D. Buckley, C. O'Dwyer, J. Electrochem. Soc 2014, 161, A1321.

[28] P. Jinshun, T. Seiji, K. Shigemi, Jpn. J. Appl. Phys. 1998, 37, 6519.

[29] C. V. Ramana, S. Utsunomiya, R. C. Ewing, U. Becker, Solid State Commun. 2006, 137, 645.

[30] Y. Zhang, M. Fan, X. Liu, C. Huang, H. Li, Eur. J. Inorg. Chem. 2012, 2012, 1650.

[31] L. Zeng, C. Zheng, J. Xi, H. Fei, M. Wei, Carbon 2013, 62, 382.

[32] A. Odani, V. G. Pol, S. V. Pol, M. Koltypin, A. Gedanken, D. Aurbach, Adv. Mater. 2006, 18, 1431.

[33] Y. Wang, H. J. Zhang, A. S. Admar, J. Luo, C. C. Wong, A. Borgna, J. Lin, RSC Adv. 2012, 2, 5748.

[34] X. Li, J. Fu, Z. Pan, J. Su, J. Xu, B. Gao, X. Peng, L. Wang, X. Zhang, P. K. Chu, J. Power Sources 2016, 331, 58.

[35] Y. Dong, R. Ma, M. Hu, H. Cheng, J.-M. Lee, Y. Y. Li, J. A. Zapien, J. Power Sources 2014, 261, 184.

[36] E. Armstrong, D. McNulty, H. Geaney, C. O'Dwyer, ACS Appl. Mater. Interfaces 2015, 7, 27006.

[37] Y. Tang, Y. Zhang, J. Deng, J. Wei, H. L. Tam, B. K. Chandran, Z. Dong, Z. Chen, X. Chen, Adv. Mater. 2014, 26, 6111.

[38] D. McNulty, E. Carroll, C. O'Dwyer, Adv. Energy Mater. 2017, n/a.

[39] E. M. Sorensen, S. J. Barry, H.-K. Jung, J. M. Rondinelli, J. T. Vaughey, K. R. Poeppelmeier, Chem. Mater. 2006, 18, 482.

[40] G. Collins, E. Armstrong, D. McNulty, S. O'Hanlon, H. Geaney, C. O'Dwyer, Sci. Technol. Adv. Mater. 2016, 17, 563.

[41] A. Vu, Y. Qian, A. Stein, Adv. Energ. Mater. 2012, 2, 1056.

[42] L. Jiang, Y. Qu, Z. Ren, P. Yu, D. Zhao, W. Zhou, L. Wang, H. Fu, ACS Appl. Mater. Interfaces 2015, 7, 1595.

[43] H. Jiang, G. Jia, Y. Hu, Q. Cheng, Y. Fu, C. Li, Ind. Eng. Chem. Res. 2015, 54, 2960.

[44] K. E. Swider-Lyons, C. T. Love, D. R. Rolison, Solid State Ion. 2002, 152–153, 99.

[45] A. Darwiche, M. T. Sougrati, B. Fraisse, L. Stievano, L. Monconduit, Electrochem. Commun. 2013, 32, 18.

[46] S. Liang, Y. Hu, Z. Nie, H. Huang, T. Chen, A. Pan, G. Cao, Nano Energy 2015, 13, 58.

[47] L. Mai, F. Dong, X. Xu, Y. Luo, Q. An, Y. Zhao, J. Pan, J. Yang, Nano Lett. 2013, 13, 740.

[48] Y. Sun, S.-B. Yang, L.-P. Lv, I. Lieberwirth, L.-C. Zhang, C.-X. Ding, C.-H. Chen, J. Power Sources 2013, 241, 168.

[49] H. J. Song, M. Choi, J.-C. Kim, S. Park, C. W. Lee, S.-H. Hong, D.-W. Kim, Mater. Lett. 2016, 180, 243.

[50] Y. Shi, Z. Zhang, D. Wexler, S. Chou, J. Gao, H. D. Abruña, H. Li, H. Liu, Y. Wu, J. Wang, Journal of Power Sources 2015, 275, 392.

[51] D. McNulty, D. N. Buckley, C. O'Dwyer, J. Solid State Electrochem. 2016, 20, 1445.

[52] D. McNulty, H. Geaney, E. Carroll, S. Garvey, A. Lonergan, C. O'Dwyer, Mater. Res. Express 2017, 4, 025011.

[53] D. McNulty, H. Geaney, E. Armstrong, C. O'Dwyer, J. Mater. Chem. A 2016, 4, 4448.

[54] D. McNulty, H. Geaney, C. O'Dwyer, Sci. Rep. 2017, 7, 42263.

[55] G. Huang, S. Xu, S. Lu, L. Li, H. Sun, ACS Appl. Mater. Interfaces 2014, 6, 7236.

[56] Y.-M. Kang, M.-S. Song, J.-H. Kim, H.-S. Kim, M.-S. Park, J.-Y. Lee, H. K. Liu, S. X. Dou, Electrochim. Acta 2005, 50, 3667.

[57] N. Wu, Y. Zhang, Y. Wei, H. Liu, H. Wu, ACS Appl. Mater. Interfaces 2016, 8, 25361.

[58] M.-J. Lee, S. Lee, P. Oh, Y. Kim, J. Cho, Nano Lett. 2014, 14, 993.

[59] Y. Zhao, L. Peng, B. Liu, G. Yu, Nano Lett. 2014, 14, 2849.

[60] H. Meng, B. Huang, J. Yin, X. Yao, X. Xu, Ionics 2015, 21, 43.

Entry for the Table of Contents

Layout 2:

ARTICLE

David McNulty, D. Noel Buckley and Colm O'Dwyer*

Page No. – Page No.

V_2O_3 Polycrystalline Nanorod Cathode Materials for Li-ion Batteries with Long Cycle Life and High Capacity Retention
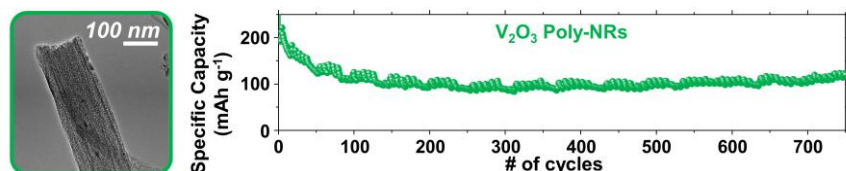
This work demonstrates the electrochemical performance of V_2O_3 polycrystalline nanorods (poly-NRs) as a cathode material for Li-ion batteries. Through galvanostatic cycling we demonstrate that poly-NRs offer excellent capacity retention over 750 cycles when cycled in a half-cell against a Li anode. We also report on the performance of V_2O_3 poly-NRs in a full Li-ion cell paired with a pre-charged Co_3O_4 inverse opal structured anode.